Computer Assisted Mechanics and Engineering Sciences, 9: 163–181, 2002.

The effect of heating/cooling on the upper-branch stability of boundary layer flows over a compliant boundary

Sandile S. Motsa[1], Jitesh S.B. Gajjar[2] and Precious Sibanda[1]
[1] *Mathematics Department, University of Zimbabwe*
P.O. Box MP 167, Mount Pleasant, Harare, Zimbabwe
[2] *Department of Mathematics, University of Manchester*
Oxford Road, Manchester M13 9PL, England

(Received May 4, 2000)

We investigate the evolution of Tollmien–Schlichting waves in boundary layers in the presence of moderate buoyancy arising from the heating or cooling of a compliant wall. We exploit the multi-deck structure of the flow in the limit of large Reynolds numbers to make an asymptotic analysis of the pertubed flow, along the upper-branch of the neutral stability curve, to derive linear neutral results. These results are discussed and are compared to rigid wall results. Also, a brief parametric study, based on the linear neutral results, is presented and the results are discussed.

Keywords: linear stability, heating and cooling, compliant surface

1. Introduction

Laminar–turbulent transition in wall flows is of great technological significance since delay in transition can result in considerable drag reduction. The study of instabilitites that occur in any fluid flow problem helps in the understanding of transition, and the supression of instability waves results in considerable transition postponement leading to significant drag reduction. Most experimental and theoretical studies in hydrodynamic stability are aimed at: identifying all possible modes of instability, finding all factors which influence transition or stability and seeking ways to delay transition, hence reduce drag. Some of the methods influencing the stability of boundary layer flow over rigid surfaces include: injection [18], suction [11], heating or cooling [19] and the use of compliant boundaries [2, 3]. In this paper we look at the combined effect of compliant boundaries and heating/cooling on the linear stability of accelerating boundary layers.

Boundary layer flows over a compliant surfaces are susceptible to a variety of instabilities which can be divided into two broad classes: Tollmien–Schlichting instabilities (TSI) and flow-induced surface instabilities (FISI). This classification was used by Carpenter and Garrad [2, 3]. The TSI are similar to the ones which exist in flows over rigid surfaces but are now modified by the presence of the compliant surface. Some of the instabilities which fall into the class of FISI are divergence and travelling wave flutter (TWF) instability. Sometimes the TWF and the TSI interact and coalesce to form a stronger instability [3].

There is now ample evidence from linear stability theory [2–5, 12, 20] that certain types of compliant surfaces are capable of producing significant transition delays through the attenuation of the TSI. In fact it has been shown that as wall compliance increases, the growth of the TSI is progressively suppressed. However, the presence of FISI frustrates the transition-delaying capability of the compliant surface [3]. In view of this fact, the focus of most researchers has shifted from trying to establish whether or not compliant surfaces delay transition through the reduction of the TSI. Instead, the factors limiting the transition-delaying performance and properties giving the optimal performance of compliant surfaces are now being sought see for example [6].

In this paper we use the self-consistent approach of Smith and Bodonyi [16, 17] to look into the effect of heating/cooling in accelerating boundary layers over compliant surfaces. The work presented here is in the same spirit as the work of Motsa et al. [14] who investigated the effect of bouyancy on channel flows with compliant boundaries. Here we have extended the work to boundary layer flows [1], developed an asymptotic theory, also in the spirit of Smith and Bodonyi [16, 17], for high Reynolds number flows to take into account the FISI. An important conclusion which can be drawn from the work of Carpenter and Gajjar [1] is that the asymptotic theory gives accurate results for the hydroelastic instabilities (FISI), and also gives a reliable, albeit qualitative, guide to the effects of wall compliance on the Tollmien–Schlichting waves. With this in mind, in this paper we address the TSI but we further extend the original problem [2] by introducing another complication — heating/cooling. It is worth mentioning here that not much research has been done on boundary layer flow over compliant surfaces with heat transfer. The effect of heating/cooling of boundary layers over compliant surfaces may have important applications in marine biology and naval engineering. For instance, it has been conjectured that laminarization of the boundary layer by body heat is responsible for the seemingly low drag of the porpoise [19].

The effect of introducing heat transfer in the upper-branch stability of Tollmien–Schlichting waves in boundary layer flow over rigid surfaces has been considered by Gajjar and Cole [8], Gajjar [7] in compressible flows, and Mureithi et al. [15], in incompressible flows. The work [15] was concerned with the effect of increasing the level of buoyancy on the upper-branch Tollmien–Schlichting waves. It was shown that for moderate thermal stratification the five-zone disturbance structure of Smith and Bodonyi [17] remained unaltered. However, as the buoyancy was increased to $O(Re^{1/2})$, where Re is the Reynolds number, the five-zone structure collapsed into a two layered structure with the disturbances now governed by the Taylor–Goldstein equation. In this work, we have restricted ourselves to the case of moderate buoyancy, in which case the five-zone structure is retained (even in the presence of a compliant boundary).

The outline of the paper is as follows: in Section 2 we outline the general mathematical formulation of the linear stability problem of boundary layer flow over a heated/cooled compliant surface. In Section 3 we present the disturbance structure and give the appropiate expansions in each region from which we derive the disturbance solutions. In Section 4 we derive the eigenrelations giving the linear neutral results and in Section 5 we give a discussion of the results. In Section 6 we give a summary of our findings.

2. Mathematical formulation

2.1. General formulation

The equations governing a two-dimensional incompressible fluid flowing over a heated/cooled compliant plate expressed in dimensionless form are, under a Boussinesq type approximation, given by

$$\frac{\partial u}{\partial x} + \frac{\partial v}{\partial y} = 0, \tag{1}$$

$$\frac{Du}{Dt} = -\frac{\partial p}{\partial x} - \frac{1}{Re}\left(\frac{\partial \sigma_{yx}}{\partial y} + \frac{\partial \sigma_{xx}}{\partial x}\right), \tag{2}$$

$$\frac{Dv}{Dt} = -\frac{\partial p}{\partial y} - \frac{1}{Re}\left(\frac{\partial \sigma_{yy}}{\partial y} + \frac{\partial \sigma_{yx}}{\partial x}\right) - \frac{\alpha g L}{U_\infty^2}[\theta_\infty - \theta_*] + G\theta, \tag{3}$$

$$\frac{D\theta}{Dt} = \frac{1}{RePr}\left(\frac{\partial^2 \theta}{\partial x^2} + \frac{\partial^2 \theta}{\partial y^2}\right) + 2\mu\frac{Ec}{Re}\left[\left(\frac{\partial u}{\partial x}\right)^2 + \left(\frac{\partial v}{\partial y}\right)^2\right] + \mu\frac{Ec}{Re}\left(\frac{\partial v}{\partial x} + \frac{\partial u}{\partial y}\right)^2, \tag{4}$$

where σ_{xx}, σ_{yy} and σ_{yx} are defined by

$$\sigma_{yx} = -\mu\left(\frac{\partial u}{\partial y} + \frac{\partial v}{\partial x}\right), \qquad \sigma_{yy} = -2\mu\frac{\partial v}{\partial y}, \qquad \sigma_{xx} = -2\mu\frac{\partial u}{\partial x}, \qquad \frac{D}{Dt} = \frac{\partial}{\partial t} + u\frac{\partial}{\partial x} + v\frac{\partial}{\partial y}.$$

Also, μ is the coefficient of dynamic viscosity, p is the pressure, θ is the temperature, g is the gravity constant, x and y are the streamwise and normal coordinates respectively, u and v are the streamwise and normal velocity components respectively and t is time.

Equations (1)–(4) have been nondimensionalized by making the following substitutions,

$$(x', y') = L(x, y), \qquad (u', v') = U_\infty(u, v), \qquad p' = \rho_* U_\infty^2 p, \qquad \mu' = \mu_*\mu, \qquad t' = (L/U_\infty)t,$$

$$\theta = \frac{\theta' - \theta_\infty}{\theta_* - \theta_\infty},$$

where the primes denote dimensional quantities, the asterisks refer to the values of the quantities at $y = 0$, the infinity subscript refers to the free stream values and L is taken to be a characteristic length measured from the plate's leading edge.

The nondimensional constants appearing in the above equations are the Prandtl number Pr, the Reynolds number Re and the Eckert number Ec given in turn by

$$Pr = \frac{c_p^* \mu_*}{k_*}, \qquad Re = \frac{U_\infty L \rho_*}{\mu_*}, \qquad Ec = \frac{U_\infty^2}{c_p^*(\theta_* - \theta_\infty)}.$$

Also, $G = GrRe^{-2}$, where Gr is the Grasshof number defined by

$$Gr = \frac{g\alpha L^3 \rho_*^2}{\mu^2}(\theta_* - \theta_\infty),$$

where c_p^* is the specific heat capacity at constant pressure, k_* is the thermal conductivity and α is the coefficient of volume expansion. We also assume that the viscosity–temperature relation is governed by the Chapman's Law

$$\mu = C\theta \tag{5}$$

where C is a constant given by $C = \mu_*/\theta_*$.

2.2. Wall model and boundary conditions

The compliant wall is modelled as a spring backed elastic plate (see for example [2]). Assuming that the motion of the compliant wall is restricted only to the vertical direction and taking vertical displacement to be η', the mechanical fluid pressure $\Delta p'$ due to η' is given by

$$\Delta p' = T'\frac{\partial^2 \eta'}{\partial x'^2} - \rho_m b'\frac{\partial^2 \eta'}{\partial t'^2} - d'\frac{\partial \eta'}{\partial t'} - B'\frac{\partial^4 \eta'}{\partial x'^4} - K'\eta'. \tag{6}$$

The wall parameters are: T' tension, ρ_m density of the plate material, b' the plate thickness, d' damping coefficient, B' the flexural rigidity of the plate and K' is the equivalent spring stiffness. We non-dimensionalize Eq. (6) by making the following substitutions,

$$x = \frac{x'}{L}, \qquad \eta = \frac{\eta'}{L}, \qquad t = \frac{t' U_\infty}{L}, \qquad \delta p = \frac{\delta p'}{\rho_* U_\infty^2}, \qquad \theta = \frac{\theta' \rho_* L}{\mu_*^2},$$

$$K = \frac{K' L^3 \rho_*}{\mu_*^2}, \qquad M = \frac{\rho_m b'}{\rho_* L}, \qquad d = \frac{d' L}{\mu_*}, \qquad B = B'\rho_*\mu_* L,$$

to obtain

$$\Delta p = \frac{T}{Re^2}\frac{\partial^2 \eta}{\partial x^2} - M\frac{\partial^2 \eta}{\partial t^2} - \frac{d}{Re}\frac{\partial \eta}{\partial t} - \frac{B}{Re^2}\frac{\partial^4 \eta}{\partial x^4} - \frac{K\eta}{Re^2}. \tag{7}$$

At the compliant wall, the boundary condition for the flow is

$$u = 0, \quad v = \frac{\partial \eta}{\partial t} \qquad \text{at} \quad y = \eta(x,t). \tag{8}$$

We shall use an isothermal boundary condition for the temperature at the compliant surface, that is we suppose that the temperature at the wall is prescribed as θ_{BW}, hence the temperature boundary condition is

$$\theta = \theta_{BW} \qquad \text{at} \quad y = \eta(x,t). \tag{9}$$

In the far field limit we assume that the velocity and temperature approach their free stream values.

In the limit as $Re \to \infty$, the basic boundary layer takes the form

$$u = U_B(x,Y) + \cdots, \qquad v = Re^{-1/2}V_B(x,Y) + \cdots, \qquad \theta = \theta_B(x,Y) + \cdots, \qquad p = P_B, \tag{10}$$

with $Y = Re^{1/2}y$ being the boundary layer coordinate. For general accelerating boundary layers, the basic velocity profile $U_B(x,Y)$ and the temperature profile $\theta_B(x,Y)$ have the following additional properties,

$$U_B \sim \lambda_1 Y + \lambda_2 Y^2 + \cdots \qquad \text{as} \quad Y \to 0,$$
$$\theta_B \sim R_0 + R_1 Y + R_2 Y^2 + \cdots \qquad \text{as} \quad Y \to 0,$$

and in the far-field limit we have

$$U_B \to 1, \quad \theta_B \to 0 \qquad \text{as} \quad Y \to \infty$$

where λ_2 and λ_1 are the curvature and skin friction respectively. The coefficients R_0, R_1 and R_2 are heat transfer coefficients.

3. Disturbance structure

In this work we adopt the five-zone asymptotic structure of Smith and Bodonyi [17] to investigate the stability of general accelerating boundary layers along the upper-branch of the neutral stability curve. The five regions (see Fig. 1) are: the main part of the boundary layer R1 of thickness $O(Re^{-1/2})$, a thinner inviscid adjustment region R2, of thickness $O(Re^{-7/12})$, containing the critical layer region R3, the viscous wall layer R4 of thickness $O(Re^{-2/3})$ and finally, the outer potential flow region R5 of thickness $O(Re^{-5/12})$. We restrict our attention to linear stability and to this end we introduce infinitesimal disturbances of size δ ($\ll 1$) to the basic flow. Smith and Bodonyi [17] found that linear stability theory holds for disturbance sizes δ less than $O(Re^{-7/36})$. It is only when δ rises to, and beyond, $O(Re^{-7/36})$ that nonlinearity comes into play.

The streamwise and temporal variations of the disturbances depend on X and τ, where $x = \epsilon^5 X$, $t = \epsilon^4 \tau$ with $\epsilon = Re^{-1/12}$. The free compliant surface is in the boundary layer and thus is of $O(\epsilon^6)$. The disturbances are taken to be in the form of a modulated wave-train, periodic in X, and we replace the derivatives $\partial/\partial x$ and $\partial/\partial t$ by $\epsilon^{-5}(\alpha_0 + \epsilon\alpha_1 + \cdots)\partial/\partial X$ and $-\epsilon^{-4}(\sigma_0 + \epsilon\sigma_1 + \cdots)\partial/\partial X$, where α_i, σ_i ($i \gg 0$) are unknown constants of $O(1)$ and are taken to be real so that we only consider neutrally stable conditions. Here we have expanded the wavenumber α and the frequency σ as

$$\alpha = \epsilon^{-5}(\alpha_0 + \epsilon\alpha_1 + \cdots), \qquad \sigma = -\epsilon^{-4}(\sigma_0 + \epsilon\sigma_1 + \cdots),$$

because we are interested in wavenumbers of $O(\epsilon^5)$ and frequencies of $O(\epsilon^4)$ respectively.

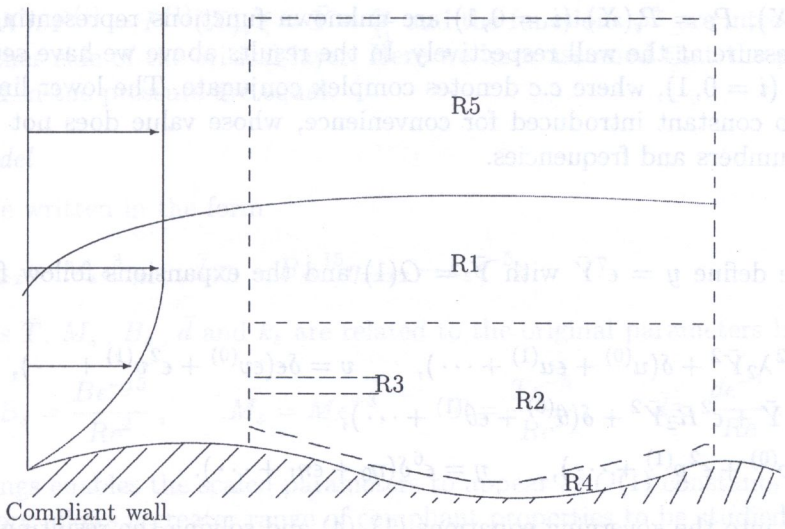

Fig. 1. Schematic sketch of multi-deck boundary layer structure

The essential difference between the current work and that of Smith and Bodonyi [17] arises from the introduction of compliance and the contributions due to temperature changes. The presence of wall compliance makes the current work different from that of Mureithi et al. [15]. The analysis of [15] showed that in the presence of strong buoyancy forces, the five-zone structure is altered. However, for moderate buoyancy, up to $O(\epsilon^{-5})$, the five-zone structure persists with some minor modifications. Throughout this work, unless otherwise stated, we set $G = \epsilon^{-5}G_0$, where G_0 is of $O(1)$. The appropiate expansions and solutions in each region are as follows:

Region R1

$$\begin{aligned} u &= U_B + \delta(u_0 + \epsilon u_1 + \cdots), & v &= \delta(\epsilon v_0 + \epsilon^2 v_1 + \cdots) \\ \theta &= \theta_B + \delta(\theta_0 + \epsilon\theta_1 + \cdots), & p &= p_B + \delta(\epsilon p_0 + \epsilon^2 p_1 + \cdots) \end{aligned} \tag{12}$$

Here, we have defined $y = \epsilon^6 Y$ where $Y = O(1)$. Substituting (12) in the governing equations (1)–(4) and solving the resulting equations yields the following solutions,

$$u_0 = A_0 U_{BY}, \qquad v_0 = -\alpha_0 A_{0X} U_B, \qquad \theta_0 = A_0 \theta_{BY}, \qquad p_0 = P_0 + G_0 A_0 (\theta_B - R_0). \tag{13}$$

At the next order, the results are:

$$v_1 = -\alpha_0 A_{1X} U_B + \alpha_0 c_0 A_{0X} + \alpha_0 U_B \int_{Y_0}^{Y} \frac{P_{0X}}{U_B^2}\,\mathrm{d}Y + \alpha_0 U_B G_0 A_{0X} \int_{Y_0}^{Y} \frac{(\theta_B - R_0)}{U_B^2}\,\mathrm{d}Y, \tag{14}$$

$$\begin{aligned} u_1 = {} & -\frac{\alpha_1}{\alpha_0} A_0 U_{BY} + A_1 U_{BY} - U_{BY} \int_{Y_0}^{Y} \frac{P_0}{U_B^2}\,\mathrm{d}Y - \frac{P_0}{U_B} - U_{BY} G_0 A_0 \int_{Y_0}^{Y} \frac{(\theta_B - R_0)}{U_B^2}\,\mathrm{d}Y \\ & - G_0 A_0 \frac{(\theta_B - R_0)}{U_B}, \end{aligned} \tag{15}$$

$$\theta_1 = -\frac{\alpha_1}{\alpha_0} A_0 \theta_{BY} + A_1 \theta_{BY} - \theta_{BY} \int_{Y_0}^{Y} \frac{P_0}{U_B^2}\,\mathrm{d}Y - \theta_{BY} G_0 A_0 \int_{Y_0}^{Y} \frac{(\theta_B - R_0)}{U_B^2}\,\mathrm{d}Y, \tag{16}$$

$$\begin{aligned} p_1 = {} & P_1 - \alpha_0^2 A_0 \int_0^Y U_B^2\,\mathrm{d}Y + G_0 \left(A_1 - \frac{\alpha_1}{\alpha_0} A_0 \right) \theta_B \\ & - G_0 \int_0^Y \theta_{BY} \left(\int_{Y_0}^{Y_1} \frac{[P_0 + G_0 A_0 (\theta_B - R_0)]}{U_B^2}\,\mathrm{d}Y_1 \right) \mathrm{d}Y, \end{aligned} \tag{17}$$

where $A_i = A_i(X)$, $P_i = P_i(X)$ $(i = 0, 1)$ are unknown functions representing the displacement effect and the pressure at the wall respectively. In the results above we have set $A_i = \bar{A}_i e^{iX} + c.c$, $P_i = \bar{P}_i e^{iX} + c.c$ $(i = 0, 1)$, where $c.c$ denotes complex conjugate. The lower limit of the integrals, Y_0, is a non zero constant introduced for convenience, whose value does not affect the eventual results for wavenumbers and frequencies.

Region R2

In this region we define $y = \epsilon^7 \bar{Y}$ with $\bar{Y} = O(1)$ and the expansions follow from the expansion in R1,

$$\begin{aligned} u &= \epsilon\lambda_1\bar{Y} + \epsilon^2\lambda_2\bar{Y}^2 + \delta(u^{(0)} + \epsilon u^{(1)} + \cdots), \qquad v = \delta\epsilon(\epsilon v^{(0)} + \epsilon^2 v^{(1)} + \cdots), \\ \theta &= R_0 + \epsilon R_1\bar{Y} + \epsilon^2 R_2\bar{Y}^2 + \delta(\theta^{(0)} + \epsilon\theta^{(1)} + \cdots), \\ p &= p_B + \delta(\epsilon p^{(0)} + \epsilon^2 p^{(1)} + \cdots), \qquad \eta = \epsilon^6\delta(\eta_0 + \epsilon\eta_1 + \cdots). \end{aligned} \tag{18}$$

Substituting (18) into the governing equations (1)–(4) and solving the resulting equations gives

$$u^{(0)} = \lambda_1 A_0\,, \qquad v^{(0)} = -\frac{\alpha_0 p_X^{(0)}}{\lambda_1} - \alpha_0 A_{0X}\lambda_1\xi, \qquad \theta^{(0)} = R_1\left(A_0 + \frac{p^{(0)}}{\lambda_1^2\xi}\right), \qquad p^{(0)} = P^{(0)}. \tag{19}$$

Using the boundary condition (8) gives

$$P^{(0)} = c_0\lambda_1(A_0 + \eta_0).$$

At the next order we obtain

$$\begin{aligned} v^{(1)} &= -\frac{1}{\lambda_1}\left[\alpha_0 P_X^{(1)} + \alpha_1 c_0\lambda_1(A_{0X} + \eta_{0X}) - \alpha_0 c_1\lambda_1 A_{0X}\right] - \bar{A}_{1X}\alpha_0\xi\lambda_1 - \frac{\alpha_0 G_0 R_1 c_0 A_{0X}}{\lambda_1^2} \\ &\quad - \alpha_0\lambda_2 A_{0X}\left(\xi^2 + 2\frac{c_0}{\lambda_1}\xi\left\{\ln|\xi| + \phi^{\pm}\right\} - \frac{c_0^2}{\lambda_1^2}\right) - \frac{2\lambda_2\alpha_0 c_0\eta_{0X}}{\lambda_1}\left(\xi\left\{\ln|\xi| + \phi^{\pm}\right\} - \frac{c_0}{\lambda_1}\right) \\ &\quad + \frac{\alpha_0 G_0 R_1}{\lambda_1}\left(A_{0X}\xi\{\ln|\xi| + \phi^{\pm}\} - \frac{c_0}{\lambda_1}(A_{0X} + \eta_{0X})(\{\ln|\xi| + \phi^{\pm}\} + 1)\right), \end{aligned} \tag{20}$$

$$\begin{aligned} u^{(1)} &= \lambda_2 A_0\left(2\xi + 2\frac{c_0}{\lambda_1}\left[1 + \{\ln|\xi| + \phi^{\pm}\}\right]\right) - \frac{2\lambda_2 c_0\eta_0}{\lambda_1}\left(1 + \{\ln|\xi| + \phi^{\pm}\}\right) - \frac{\alpha_1\lambda_1 A_0}{\alpha_0} + \bar{A}_1\lambda_1 \\ &\quad - \frac{G_0 R_1}{\lambda_1}\left(A_0(1 + \{\ln|\xi| + \phi^{\pm}\} - \frac{c_0}{\lambda_1}(A_0 + \eta_0)\xi^{-1}\right), \end{aligned} \tag{21}$$

$$\begin{aligned} \theta^{(1)} &= -\frac{R_1\lambda_2}{\lambda_1\xi}\left(\xi + \frac{c_0}{\lambda_1}\right)^2\left(A_0 + \frac{c_0(\eta_0 + A_0)}{\lambda_1\xi}\right) - \frac{\alpha_1 R_1}{\alpha_0}\left(A_0 + \frac{c_0(A_0 + \eta_0)}{\lambda_1\xi}\right) \\ &\quad + \frac{R_1}{\alpha_0\lambda_1^2\xi}\left(\alpha_0 P^{(1)} + \alpha_1 c_0\lambda_1(A_0 + \eta_0) - \alpha_0 c_1\lambda_1 A_0\right) + \frac{c_1 R_1}{\lambda_1\xi}\left(A_0 + \frac{c_0(A_0 + \eta_0)}{\lambda_1\xi}\right) \\ &\quad + \frac{R_1\lambda_2 A_0}{\lambda_1\xi}\left(\xi^2 + 2\frac{c_0}{\lambda_1}\xi\left\{\ln|\xi| + \phi^{\pm}\right\} - \frac{c_0^2}{\lambda_1}\right) + \frac{2R_1\lambda_2 c_0\eta_0}{\lambda_1^2\xi}\left(\xi\left\{\ln|\xi| + \phi^{\pm}\right\} - \frac{c_0}{\lambda_1}\right) \\ &\quad + R_1\bar{A}_1 + \frac{2R_2}{\alpha_0\lambda_1}\left(1 + \frac{c_0}{\lambda_1\xi}\right)\left(\frac{\alpha_0\bar{p}_{0X}}{\lambda_1} + \alpha_0\lambda_1 A_{0X}\xi\right) \\ &\quad - \frac{G_0 R_1^2}{\lambda_1^2}\left[A_0\{\ln|\xi| + \phi^{\pm}\} - \frac{c_0 A_0}{\lambda_1}\xi^{-1} - \frac{c_0}{\lambda_1}(A_0 + \eta_0)(\{\ln|\xi| + \phi^{\pm}\} + 1)\xi^{-1}\right], \end{aligned} \tag{22}$$

$$p^{(1)} = P^{(1)} + G_0 R_1\left[A_0(\xi + \frac{c_0}{\lambda_1}) + \frac{c_0}{\lambda_1}(A_0 + \eta_0)\{\ln|\xi| + \phi^{\pm}\}\right], \tag{23}$$

where $P^{(0)} = P^{(0)}(X)$, $P^{(1)} = P^{(1)}(X)$, $\xi = \bar{Y} - \frac{c_0}{\lambda_1}$ and the functions $\phi^{\pm}$ are introduced to connect the solutions on either side of the critical layer. Here we have assumed that the phase shift in the normal velocity and in the pressure are equal.

Compliant wall model

Equation (7) can be written in the form

$$\Delta p = p' = \bar{T}\epsilon^5\eta_{xx} - M_s\epsilon^3\eta_{tt} - \bar{d}\epsilon\eta_t - B_s\epsilon^{15}\eta_{xxxx} - k_s\epsilon^{-5}\eta \tag{24}$$

where the constants $\bar{T}$, M_s, B_s, $\bar{d}$ and k_s are related to the original parameters by

$$k_s = \frac{k\epsilon^5}{Re^2}, \qquad B_s = \frac{B\epsilon^{-15}}{Re^2}, \qquad M_s = M\epsilon^{-3}, \qquad \bar{T} = \frac{T\epsilon^{-5}}{Re^2}, \qquad \bar{d} = \frac{d\epsilon^{-1}}{Re}.$$

This choice of scalings enables the scaled parameters to appear as $O(1)$ constants in the eigenvalue relation and therefore allows a greater range of compliant properties to be studied. The fluctuating pressure at the wall p^* and the vertical displacement η are respectively expanded as

$$p^* = \delta(\epsilon\tilde{p_0} + \epsilon^2\tilde{p}_1 + \cdots), \qquad \eta = \delta\epsilon^6(\eta_0 + \epsilon\eta_1 + \cdots). \tag{25}$$

Setting $\eta_i = \tilde{\eta}_i e^{iX}$ (for $i = 0, 1, \ldots$) and using Eqs. (24) and (25) we get

$$\tilde{p}_0 = s_0\eta_0\,. \tag{26}$$

At the next order we obtain

$$\tilde{p}_1 = \tilde{P}_1 = s_0\eta_1 + 2\bar{T}\alpha_0\alpha_1\eta_{0XX} + \bar{d}\alpha_0 c_0\eta_{0X} - 2\bar{M}\alpha_0 c_0(\alpha_0 c_1 + \alpha_1 c_0)\eta_{0XX} + 4\bar{B}\alpha_0^3\alpha_1\eta_{0XX} \tag{27}$$

where

$$s_0 = -\bar{T}\alpha_0^2 + M_s\alpha_0^2 c_0^2 - B_s\alpha_0^4 - k_s\,.$$

Region R4

In this region, $y = \eta(x,t) + \epsilon^8 z$, where z is an $O(1)$ coordinate and the flow expansions are

$$\begin{aligned} u &= U_B + \delta\tilde{u}_0 + \cdots, & v &= \eta_t(x,t) + \delta\epsilon^3\tilde{v}_0 + \cdots, \\ \theta &= \theta_B + \delta\tilde{\theta}_0 + \cdots, & p &= p_B + \delta\epsilon\tilde{p}_0 + \cdots. \end{aligned} \tag{28}$$

Substituting these expansions into the governing equations (1)–(4) and then solving the resulting disturbance equations, subject to the boundary conditions at the compliant wall and the matching (as $z \to \infty$) with the results from R2 (as $\bar{Y} \to 0$), yields

$$\tilde{u}_0 = \frac{\tilde{p}_0}{c_0}(1 - e^{-mz}) - \lambda_1\eta_0\,, \tag{29}$$

$$\tilde{v}_0 = -i\alpha_0\left(\frac{\tilde{p}_0}{c_0} - \lambda_1\eta_0\right)z - \frac{i\alpha_0\tilde{p}_0}{mc_0}(e^{-mz} - 1), \tag{30}$$

$$\tilde{\theta}_0 = -R_1\eta_0\,, \tag{31}$$

where

$$m = \left(\frac{\alpha_0 c_0}{CR_0}\right)^{\frac{1}{2}} e^{-i\frac{\pi}{4}}.$$

The above results were obtained by looking for solutions of the form $\tilde{u}_0 = \bar{u}_0 e^{iX}$, $\tilde{v}_0 = \bar{v}_0 e^{iX}$, etc.

Region R5

In this region we define $y = \epsilon^5 \hat{y}$, where $\hat{y} = O(1)$ and the appropiate expansions follow from Eq. (12) in the limit $Y \to \infty$ and are given by

$$\begin{aligned} u &= 1 + \delta\epsilon(\hat{u}_0 + \epsilon\hat{u}_1 + \cdots), & v &= \delta\epsilon(\hat{v}_0 + \epsilon\hat{v}_1 + \cdots), \\ \theta &= \delta\epsilon(\hat{\theta}_0 + \epsilon\hat{\theta}_1 + \cdots), & p &= p_B + \delta\epsilon(\hat{p}_0 + \epsilon\hat{p}_1 + \cdots). \end{aligned} \tag{32}$$

From these expansions we obtain the following solutions,

$$\hat{p}_0 = \hat{P}_0 e^{-\alpha_0 \hat{y}}, \qquad \hat{v}_0 = -i\hat{P}_0 e^{-\alpha_0 \hat{y}}, \qquad \hat{u}_0 = -\hat{P}_0 e^{-\alpha_0 \hat{y}}, \qquad \hat{\theta}_0 = B_0\,, \tag{33}$$

where $\hat{P}_0$ is an unknown function which describes the disturbance pressure at the outer extreme of the boundary layer. Using the temperature condition at the outer extreme of the boundary layer we find that $B_0 = 0$.

The next order solutions are

$$\begin{aligned} \hat{p}_1 &= \left[\hat{P}_1 - \alpha_1 \hat{y}\hat{P}_0\right] e^{-\alpha_0 \hat{y}}, & \hat{v}_1 &= -i\left[\hat{P}_1 - (\alpha_1 \hat{y} - c_0)\hat{P}_0\right] e^{-\alpha_0 \hat{y}}, \\ \hat{u}_1 &= -\left[\hat{P}_1 - (\alpha_1 \hat{y} - c_0)\hat{P}_0\right] e^{-\alpha_0 \hat{y}}, & \hat{\theta}_1 &= 0, \end{aligned} \tag{34}$$

where $\hat{P}_1$ is an unknown.

4. Matching of solutions and eigenrelations

4.1. Leading order eigenrelation

The matching of pressure between R1 (in the limit as $Y \to \infty$) with R5 (in the limit $\hat{y} \to 0$) yields

$$\hat{P}_0 = P_0 - G_0 A_0 R_0\,. \tag{35}$$

Matching of leading order normal velocities between R1 and R5 gives,

$$\hat{P}_0 = \alpha_0 A_0\,. \tag{36}$$

From Eqs. (35) and (36) it follows that

$$P_0 = A_0(G_0 R_0 + \alpha_0). \tag{37}$$

Next we consider the mathcing between R1 (in the limit $Y \to 0$) with R2 (in the limit $\bar{Y} \to \infty$). Matching of the pressures gives

$$p_0 = P_0 = P^{(0)} = c_0\lambda_1(A_0 + \eta_0). \tag{38}$$

Matching pressure between R2 (in the limit $\bar{Y} \to 0$) with R4 (in the limit $z \to \infty$) gives

$$p^{(0)} = \tilde{P}_0 = P^{(0)} = s_0\eta_0\,. \tag{39}$$

Combining (38) and (39) yields

$$\eta_0 = \frac{c_0\lambda_1 A_0}{s_0 - \lambda_1 c_0} \qquad \text{and} \qquad P^{(0)} = \frac{s_0 c_0 \lambda_1 A_0}{s_0 - \lambda_1 c_0}\,. \tag{40}$$

We can eliminate A_0, $\hat{P}_0$ and P_0 by combining Eqs. (37), (38) and (40) to get

$$\sigma_0 = \frac{\alpha_0(G_0 R_0 + \alpha_0)(s_0 - c_0\lambda_1)}{\lambda_1 s_0} \tag{41}$$

where $\sigma_0 = \alpha_0 c_0$.

The result of Mureithi et al. [15] may be recovered by setting $R_0 = 1$ and taking the limit $s_0 \to \infty$, corresponding to the rigid wall case, in Eq. (41).

4.2. Second order matching and eigenrelation

The matching of pressure components between R1 (as $Y \to \infty$) and R5 (as $\hat{y} \to 0$) yields

$$\hat{P}_1 = P_1 - \alpha^2 A_0 I_0 + G_0(A_1 - \frac{\alpha_1}{\alpha_0} A_0)\theta_B^\infty - G_0 J_0 A_0 \,, \tag{42}$$

where $\theta_B^\infty = \lim_{Y\to\infty} \theta_B$ and the constants I_0, J_0 (and other I_i's, J_i's for $i = 1, 2\ldots$, below) are defined in the Appendix.

Next matching the normal velocity component between region R1 and R5 at second order gives

$$-i\hat{P}_1 = ic_0\hat{P}_0 - \alpha_0 A_{1X} U_B^\infty + \alpha_0 c_0 A_{0X} + \alpha_0 U_B^\infty P_{0X} I_1 + \alpha_0 U_B^\infty G_0 A_{0X} J_1 \,, \tag{43}$$

where $U_B^\infty = \lim_{Y\to\infty} U_B$. Matching the pressure terms across regions R2 (as $\bar{Y} \to \infty$) and R1 (as $Y \to 0$) gives

$$P_1 = P^{(1)} + \frac{G_0 R_1 c_0}{\lambda_1}(A_0 + \eta_0)\phi^+ - G_0\left(A_1 - \frac{\alpha_1}{\alpha_0}\right)\theta_B^0 \,, \tag{44}$$

where $\theta_B^0 = \lim_{Y\to 0} \theta_B$. Matching of the normal velocity across regions R2 and R1 yields

$$\frac{-2\alpha_0 c_0 \lambda_2}{\lambda_1}(A_{0X} + \eta_{0X})\,\phi^+ + \frac{\alpha_0 G_0 R_1 A_{0X}}{\lambda_1}\phi^+ - \bar{A}_{1X}\alpha_0\lambda_1 = D_0 A_{0X} + G_0 E_0 A_{0X} - \alpha_0 A_{1X}\lambda_1 \,, \tag{45}$$

where the constants D_0, E_0 (and other D_i's, and E_i's for $i = 1, 2, \ldots$, below) are defined in the appendix. Matching of pressure between R2 and R4 gives

$$\tilde{p}_1 = P^{(1)} + \frac{G_0 R_0 c_0}{\lambda_1}(A_0 + \eta_0)\left\{\ln\left|\frac{c_0}{\lambda_1}\right| + \phi^-\right\}. \tag{46}$$

A matching of the normal velocity between R2 and R4 gives

$$\begin{aligned} &-\frac{1}{\lambda_1}\left(\alpha_0 P_X^{(1)} + \alpha_1 c_0\lambda_1(A_{0X} + \eta_{0X}) - \alpha_0 c_1\lambda_1 A_{0X}\right) + \frac{2\alpha_0 c_0^2\lambda_2}{\lambda_1^2}(A_{0X} + \eta_{0X})\phi^- + \alpha_0 c_0 \bar{A}_{1X} \\ &\quad + A_{0X} G_0 E_1 + A_{0X} D_1 - \frac{\alpha_0 G_0 R_1 c_0}{\lambda_1^2}(2A_{0X} + \eta_{0X})\phi^- = \frac{i\alpha_0\tilde{p}_0}{mc_0} - \sigma_1\eta_{0X} - \sigma_0\eta_{1X} \,. \end{aligned} \tag{47}$$

The relations (35)–(47) above may be used to eliminate $\bar{A}_1$, P_1, $P^{(1)}$, P_0, $\hat{P}_0$ and η_1 to obtain a relation which determines the higher-harmonic components of A_1. If we restrict our attention to the e^{iX} components, then after some algebra Eqs. (35)–(47) lead to

$$\begin{aligned} &iD_2 A_0 + iE_2 G_0 A_0 - \frac{2i\alpha_0 c_0^2\lambda_2}{\lambda_1}(A_0 + \eta_0)(\phi^+ - \phi^-) \\ &\quad - \frac{\alpha_0 c_0\lambda_1}{s_0}\left(-2i\alpha_0\alpha_1\bar{T}\eta_0 - \bar{d}\alpha_0 c_0\eta_0 + 2iM_s\alpha_0 c_0(\alpha_0 c_1 + \alpha_1 c_0)\eta_0 - 4iB_s\alpha_0^3\alpha_1\eta_0\right) \\ &\quad + \frac{i\alpha_0 c_0 G_0 R_1 A_0}{\lambda_1}(\phi^+ - \phi^-) + i\alpha_0\left(1 - \frac{c_0\lambda_1}{s_0}\right)\frac{G_0 R_1 c_0}{\lambda_1}(A_0 + \eta_0)(\phi^+ - \phi^-) \\ &\quad + i\alpha_0 c_0\lambda_1 A_1 U_B^\infty - i\alpha_0\left(1 - \frac{c_0\lambda_1}{s_0}\right)\left[\alpha_0 A_1 U_B^\infty - G_0 A_1(\theta_B^\infty - \theta_B^0)\right] - \frac{i\alpha_0\lambda_1\tilde{p}_0}{mc_0} = 0. \end{aligned} \tag{48}$$

Since $U_B^\infty = 1$, $\theta_B^\infty = 0$, $\theta_B^0 = R_0$, the coefficient of A_1 in (48) is

$$i\alpha_0 c_0\lambda_1 - i\alpha_0\left(1 - \frac{c_0\lambda_1}{s_0}\right)(\alpha_0 + G_0 R_0)$$

which is zero according to the first dispersion relation. The results for linear theory are derived by taking the jump across the critical layer, ϕ to be equal to $-i\pi$ (see for example [13]). Taking the real parts of (48) then gives

$$-\frac{\alpha_0\lambda_1^2}{\sqrt{2\bar{m}}} - \frac{d_{1r}\alpha_0^2 c_0^3\lambda_1^2}{s_0^2} = \frac{2\alpha_0 c_0^2\lambda_2\pi}{\lambda_1} - \frac{2\alpha_0 c_0 G_0 R_1\pi}{\lambda_1}\left(\frac{s_0 - c_0\lambda_1}{s_0}\right) \tag{49}$$

where d_{1r} is the real part of $\bar{d}$ and $\bar{m} = \sqrt{\alpha_0 c_0/CR_0}$. Equations (41) and (49) are the crucial eigenvalue relations which fix the neutral wavenumber to the neutral wavespeed. These relations can be solved simultaneously to give the required linear neutral results.

5. Results and discussion

The main results for this work are the eigenrelations given below,

$$-\frac{\alpha_0\lambda_1^2}{\sqrt{2\bar{m}}} - \frac{d_{1r}\alpha_0^2 c_0^3\lambda_1^2}{s_0^2} = \frac{2\alpha_0 c_0^2\lambda_2\pi}{\lambda_1} - \frac{2\alpha_0 c_0 G_0 R_1\pi}{\lambda_1}\left(\frac{s_0 - c_0\lambda_1}{s_0}\right), \tag{50}$$

$$c_0\lambda_1 s_0 = (s_0 - c_0\lambda_1)(G_0 R_0 + \alpha_0), \tag{51}$$

and where

$$s_0 = -\bar{T}\alpha_0^2 + M_s\alpha^2 c_0^2 - B_s\alpha_0^4 - k_s\,. \tag{52}$$

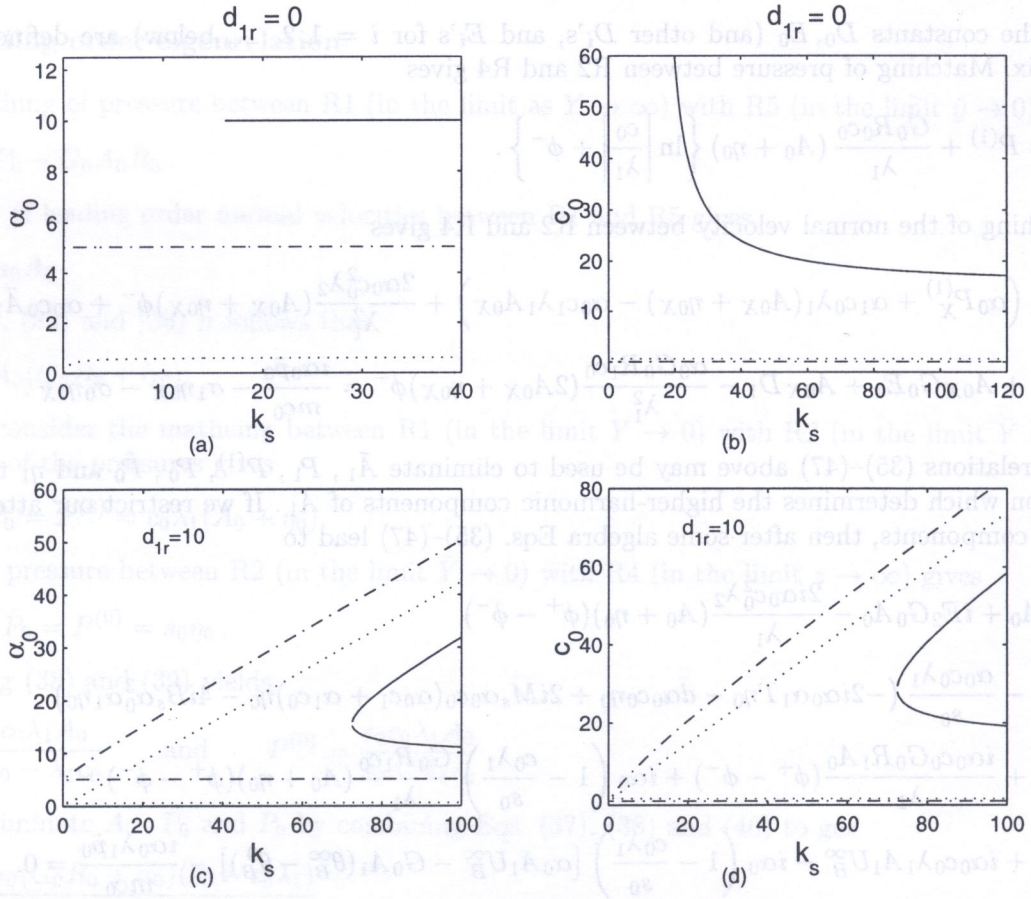

Fig. 2. (a) Linear neutral wavenumber α_0 against k_s for $d_{1r} = 0$, $G_0 = 5$ $(-)$, $G_0 = 0$ $(\cdots)$, $G_0 = -5$ $(\cdot - \cdot - \cdot)$; The values of M_s, B_s and $\bar{T}$ are all zero; (b) linear neutral phase speed c_0 against k_s with the same values of the other parameters as in (a); (c) linear neutral wavenumber α_0 against k_s for $d_{1r} = 10$, $G_0 = 5$ $(-)$, $G_0 = 0$ $(\cdots)$, $G_0 = -5$ $(\cdot - \cdot - \cdot)$ and the values of M_s, B_s and $\bar{T}$ are all zero; (d) neutral wavespeed c_0 against k_s with the same values of the other parameters as in (c)

Note that if we set $CR_0 = 1$ and take the limits $G_0 \to 0$, $s_0 \to \infty$, we recover the results of Smith and Bodonyi [17] corresponding to the case of a boundary layer flow over a flat plate in the absence of heating/cooling. For a given set of wall parameters, $\bar{T}$, k_s, M_s, B_s, d_{1r} and buoyancy parameter G_0, Eqs. (50) and (51) can be solved numerically to obtain the neutral wavenumber α_0 and wave speed c_0. In the numerical results presented in this paper, we have used the basic velocity and temperature profiles given by $U_B = y - y^2/2$ and $\theta_B = 1 - 3y/2$ respectively (these basic flow profiles were also used by Mureithi et al. [15]). This gives $\lambda_1 = 1$, $\lambda_2 = -1/2$, $R_0 = 1$ and $R_1 = -3/2$. We have also set $C = 1$. The results presented in Figs. 2–9 are for a selected set of parameters, and the general trends shown in these figures are confirmed by the analysis of the limiting cases below.

In Fig. 2a–d we show the variation of the neutral wavenumber α_0 and the neutral wave speed c_0 against k_s for a selected values of G_0 with M_s, B_s, $\bar{T}$ set equal to zero. We note that as k_s increases, the rigid wall results are recovered. When $G \geq 0$, $d_{1r} = 0$ the most pronounced deviation from the rigid wall result occurs for small values of k_s. It can be seen from Fig. 2a,b that there is a finite range of k_s where the neutral modes are absent. When the damping parameter is not equal to zero, see Fig. 2c,d, we find that as k_s increases there exist another mode (in addition to the rigid wall mode) with wavenumbers and wave speeds which increase as k_s increases.

In Fig. 3a,b we show the variation of α_0, c_0 against d_{1r} for $k_s = 100$, $G_0 = -5, 0, 5$ with all other wall parameters set to zero. From this figure we see that the rigid limit is not obtained at large values of d_{1r} for the case $G_0 = 5$. It is seen that as damping increases in the cases $G_0 \leq 0$, two distinct roots of the dispersion relation exist. One of the roots is the rigid wall solution. The

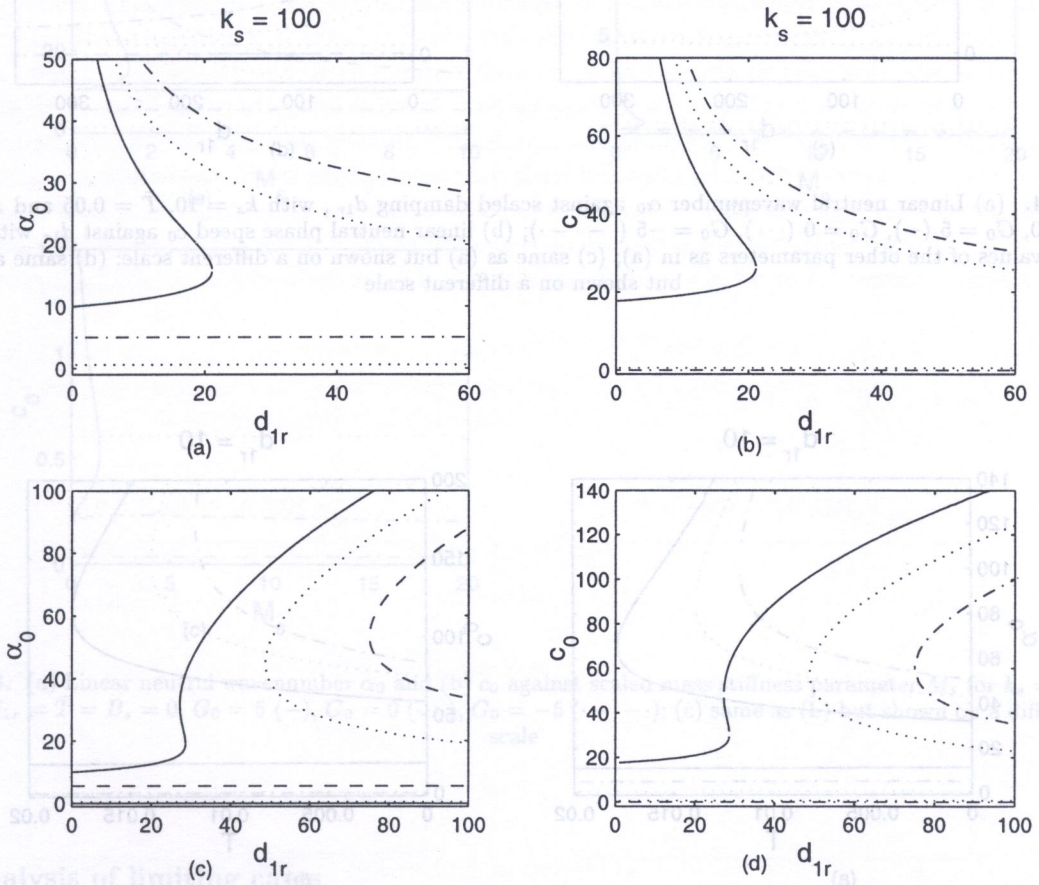

Fig. 3. (a) Linear neutral wavenumber α_0 against scaled damping d_{1r}, with $k_s = 100$ and $M_s = B_s = \bar{T} = 0$, $G_0 = 5$ $(-)$, $G_0 = 0$ $(\cdots)$, $G_0 = -5$ $(\cdot - \cdot - \cdot)$; (b) linear neutral phase speed c_0 against d_{1r} with the same values of the other parameters as in (a); (c) linear neutral α_0 and (d) c_0 against d_{1r} with $k_s = 100$, $\bar{T} = 0.05$, $M_s = B_s = 0$, $G_0 = 5$ $(-)$, $G_0 = 0$ $(\cdots)$, $G_0 = -5$ $(\cdot - \cdot - \cdot)$

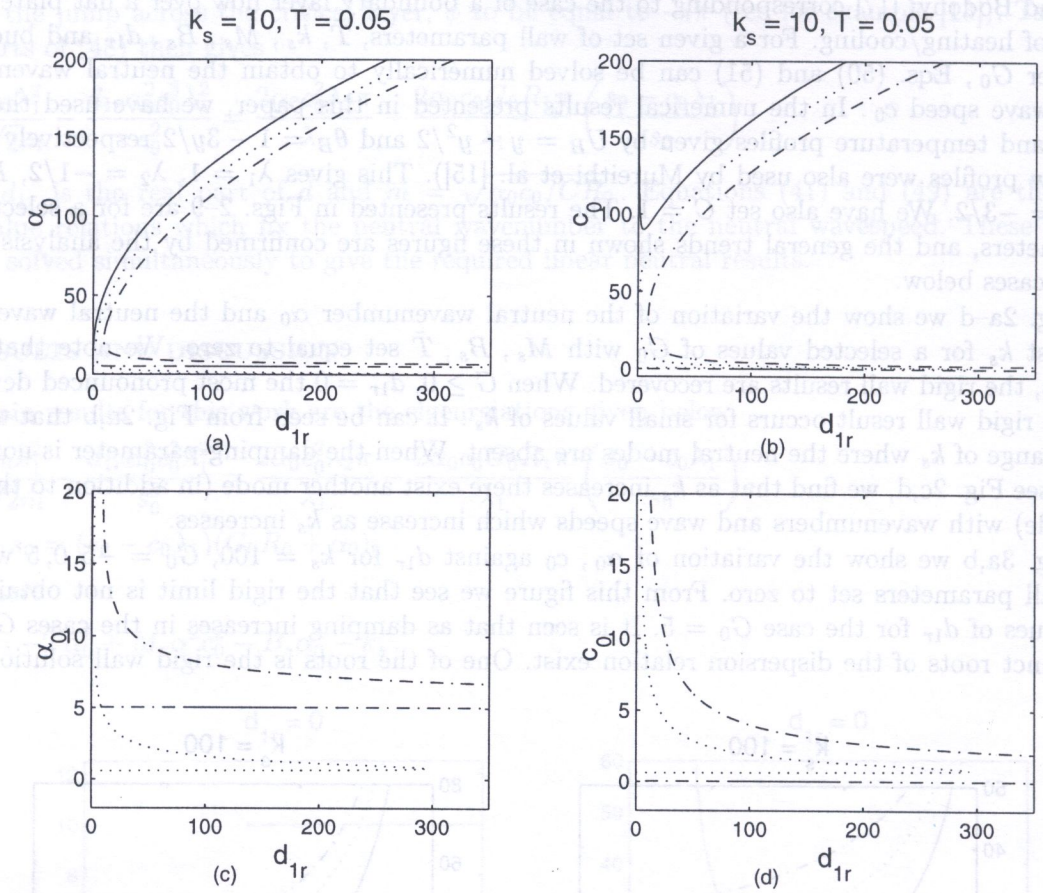

Fig. 4. (a) Linear neutral wavenumber α_0 against scaled damping d_{1r}, with $k_s = 10$, $\bar{T} = 0.05$ and $M_s = B_s = 0$, $G_0 = 5$ $(-)$, $G_0 = 0$ $(\cdots)$, $G_0 = -5$ $(\cdot - \cdot - \cdot)$; (b) linear neutral phase speed c_0 against d_{1r} with the same values of the other parameters as in (a); (c) same as (a) but shown on a different scale; (d) same as (b) but shown on a different scale

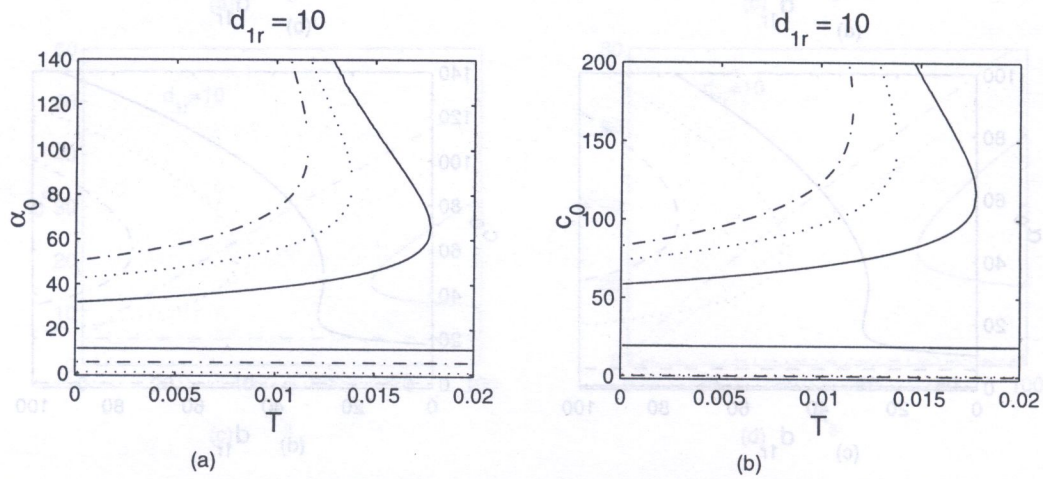

Fig. 5. (a) Linear neutral wavenumber α_0 and (b) c_0 against scaled tension parameter $\bar{T}$ with $k_s = 100$, $d_{1r} = 10$ and $M_s = B_s = 0$, $G_0 = 5$ $(-)$, $G_0 = 0$ $(\cdots)$, $G_0 = -5$ $(\cdot - \cdot - \cdot)$

other has α_0 and c_0 which decrease as d_{1r} increases. In Fig. 3c,d we show the variation of α_0 and c_0 against d_{1r} for $k_s = 100$, $G_0 = -5, 0, 5$, $\bar{T} = 0.05$ with all other wall parameters set to zero. It is seen that as damping increases in the cases $G \leq 0$, beyond a critical value of damping, three distinct roots of the dispersion relations exist. In Fig. 4a–d we show the variation of α_0 and c_0 against d_{1r} for $k_s = 10$ with all other parameters being the same as in Fig. 3c,d. It can be seen that for larger damping, the rigid wall solution dissappears and is replaced by one with much larger α_0 and enhanced wave speeds c_0 (see for example the $G_0 = 0$ mode).

In Fig. 5a,b we show some results for α_0, c_0 against the scaled tension parameter $\bar{T}$, for $d_{1r} = 10$, $k_s = 100$, $G_0 = -5, 0, 5$ with all other parameters set to zero. It can be seen that for small values of $\bar{T}$ three roots of the dispersion relations exist. As $\bar{T}$ increases, the other two roots disappear and only the rigid solution remains. In Fig. 6a–c we show α_0 and c_0 against M_s for a fixed value of k_s with all other parameters set to zero. As M_s increases there exist two distinct modes when $G_0 \leq 0$ and one mode when $G_0 > 0$. The most pronounced deviation from the rigid limit occurs at smaller values of M_s.

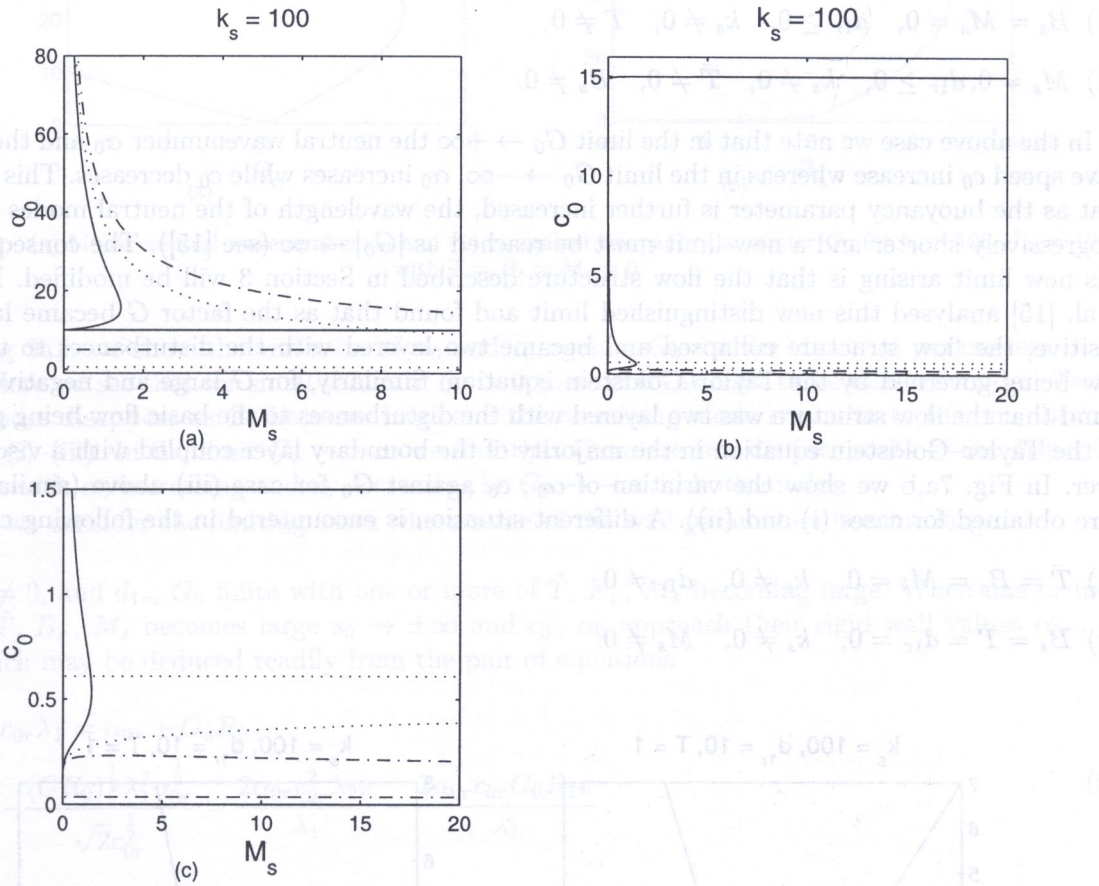

Fig. 6. (a) Linear neutral wavenumber α_0 and (b) c_0 against scaled mass stiffness parameter M_s for $k_s = 100$ with $d_{1r} = \bar{T} = B_s = 0$, $G_0 = 5$ $(-)$, $G_0 = 0$ $(\cdots)$, $G_0 = -5$ $(\cdot - \cdot - \cdot)$; (c) same as (b) but shown on a different scale

5.1. Analysis of limiting cases

In this section we present some results for the limiting behaviour of the neutral wavenumber α_0, and the neutral wavespeed c_0, as the buoyancy parameter G_0, and some of the wall parameters are increased. Firstly we consider the limiting case $G_0 \to \pm\infty$. The physical significance of the

limit $G_0 \to +\infty$ ($G_0 \to -\infty$) corresponds to increasing (decreasing) buoyancy force through, for example, an increase in wall heating (cooling).

From the eigenrelation (50) and (51) we have, in the limit $G_0 \to \infty$,

$$\alpha_0 = \left(-R_0 + \frac{R_1\lambda_1}{\lambda_2}\right) G_0 + \cdots, \qquad c_0 = \frac{R_1}{\lambda_2} G_0 + \cdots, \tag{53}$$

whereas in the limit $G_0 \to -\infty$ we get

$$\alpha_0 = -R_0 G_0 + O(G_0^{-1}), \qquad c_0 = \frac{-(CR_0)^{\frac{1}{3}}\lambda_1^2}{(8R_0R_1^2\pi^2)^{\frac{1}{3}}} G_0^{-1} + O(G_0^{-2}). \tag{54}$$

The results (53) and (54) were obtained when the following choice of parameters were used,

(i) $\bar{T} = B_s = M_s = d_{1r} = 0, \quad k_s \neq 0,$

(ii) $B_s = M_s = 0, \quad d_{1r} \geq 0, \quad k_s \neq 0, \quad \bar{T} \neq 0,$

(iii) $M_s = 0, d_{1r} \geq 0, \quad k_s \neq 0, \quad \bar{T} \neq 0, \quad B_s \neq 0.$

In the above case we note that in the limit $G_0 \to +\infty$ the neutral wavenumber α_0 and the neutral wave speed c_0 increase whereas in the limit $G_0 \to -\infty$, α_0 increases while c_0 decreases. This suggests that as the buoyancy parameter is further increased, the wavelength of the neutral modes becomes progressively shorter and a new limit must be reached as $|G_0| \to \infty$ (see [15]). The consequence of this new limit arising is that the flow structure described in Section 3 will be modified. Mureithi et al. [15] analysed this new distinguished limit and found that as the factor G became large and positive, the flow structure collapsed and became two layered with the disturbances to the basic flow being governed by the Taylor–Goldstein equation. Similarly, for G large and negative, it was found that the flow structure was two layered with the disturbances to the basic flow being governed by the Taylor–Goldstein equation in the majority of the boundary layer coupled with a viscous wall layer. In Fig. 7a,b we show the variation of α_0, c_0 against G_0 for case (iii) above (similar curves were obtained for cases (i) and (ii)). A different situation is encountered in the following cases

(iv) $\bar{T} = B_s = M_s = 0, \quad k_s \neq 0, \quad d_{1r} \neq 0,$

(v) $B_s = \bar{T} = d_{1r} = 0, \quad k_s \neq 0, \quad M_s \neq 0.$

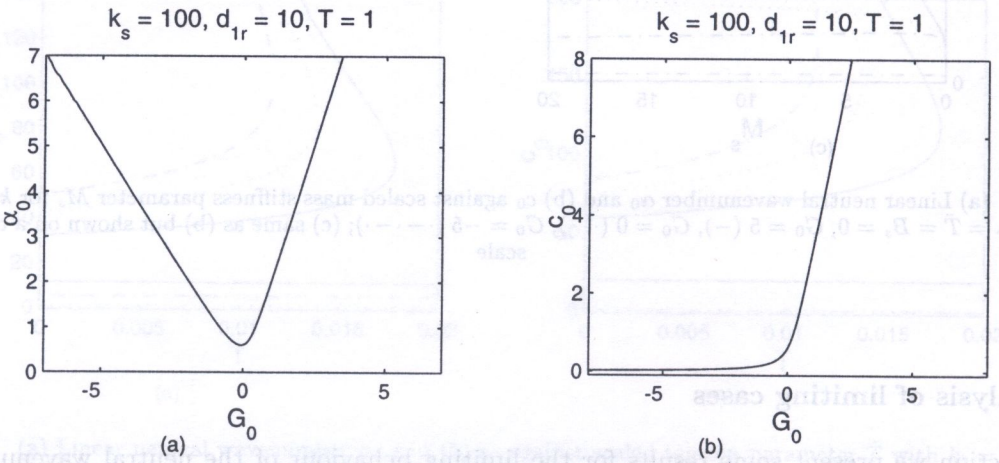

Fig. 7. (a) Linear neutral wavenumber α_0 and (b) c_0 against buoyancy parameter G_0 for $k_s = 100$, $d_{1r} = 10$, $\bar{T} = 1$ with $B_s = M_s = 0$

In Fig. 8a,b we show the variation of α_0 and c_0 against G_0 for the choice of parameters in (iv). As it can be seen from the graphs, in the limit $G_0 \to \infty$ we obtain two distinct roots of the dispersion relations. These two roots appear to merge at some finite value of G_0 beyond which no mode exists. This means that as G_0 becomes large, no new limit is obtained in this case and consequently, the inviscid modes will not be observed. In the limit $G_0 \to -\infty$ there are two distinct modes. The first mode resembles the modes of Fig. 7a,b with α_0 increasing and c_0 decreasing as $G_0 \to -\infty$ while in the other mode both α_0 and c_0 increase as $G_0 \to -\infty$.

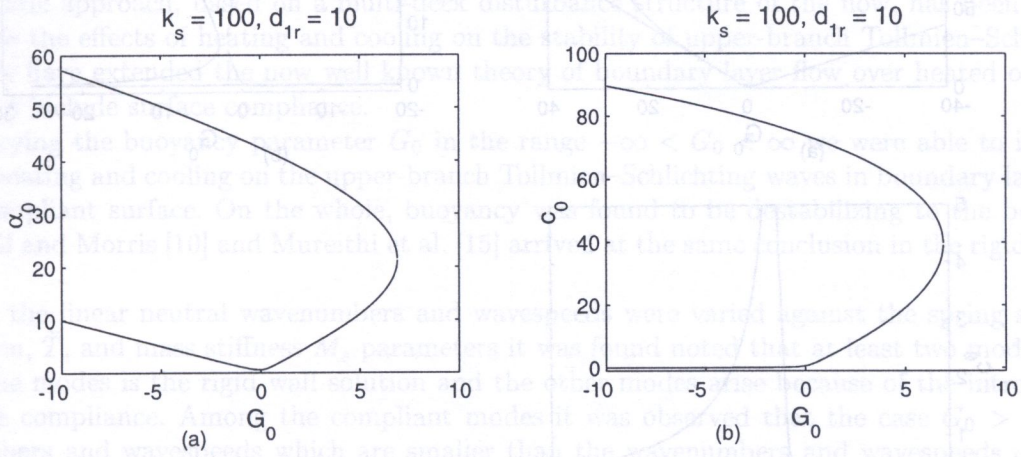

Fig. 8. (a) Linear neutral wavenumber α_0 and (b) c_0 against buoyancy parameter G_0 for $k_s = 100$, $d_{1r} = 10$ with $\bar{T} = B_s = M_s = 0$

In Fig 9a,b we show the variation of α_0 and c_0 against G_0 for the choice of parameters in (v) above. Here we see that for small values of $G_0 > 0$ there exist at least three distinct modes. Two of these modes disappear as G_0 becomes large and the remaining mode is similar to the one obtained in cases (i)–(iii). In the limit $G_0 \to -\infty$ we find that there are two distinct roots of the dispersion relations with α_0 increasing and c_0 decreasing as $G_0 \to -\infty$ in both modes.

Next we consider the limiting cases where some of the wall parameters become large.

(i) $k_s \neq 0$, and d_{1r}, G_0 finite with one or more of $\bar{T}$, B_s, M_s becoming large. When one or more of $\bar{T}$, B_s, M_s becomes large $s_0 \to \pm\infty$ and c_0, α_0 approach their rigid wall values α_{0r}, c_{0r} which may be deduced readily from the pair of equations

$$c_{0r}\lambda_1 = \alpha_{0r} + G_0 R_0 ,$$
$$-\frac{(CR_0)^{\frac{1}{2}}\lambda_1^2 \alpha_{0r}^{\frac{1}{2}}}{\sqrt{2}c_{0r}^{\frac{1}{2}}} = \frac{2\alpha_{0r}c_{0r}^2\lambda_2\pi}{\lambda_1} - \frac{2\alpha_{0r}c_{0r}G_0R_1\pi}{\lambda_1} . \tag{55}$$

Note that when we set $G_0 = 0$ in (55), we get

$$c_{0r} = \frac{\alpha_{0r}}{\lambda_1} , \qquad \alpha_{0r} = \frac{\lambda_1^{\frac{11}{6}}(CR_0)^{\frac{1}{6}}}{\sqrt{2}(-\pi\lambda_2)^{\frac{1}{3}}} ,$$

which reduces to the result of Smith and Bodonyi [17] if we set $CR_0 = 1$.

(ii) $\bar{T} = M_s = B_s = 0$, $d_{1r} = 0$, G_0 finite. If $k_s \to \infty$, then $s_0 \to -\infty$ and from the eigenrelations we can show that α_0, c_0 remain $O(1)$ and approach their rigid wall values which may be obtained from solving (55).

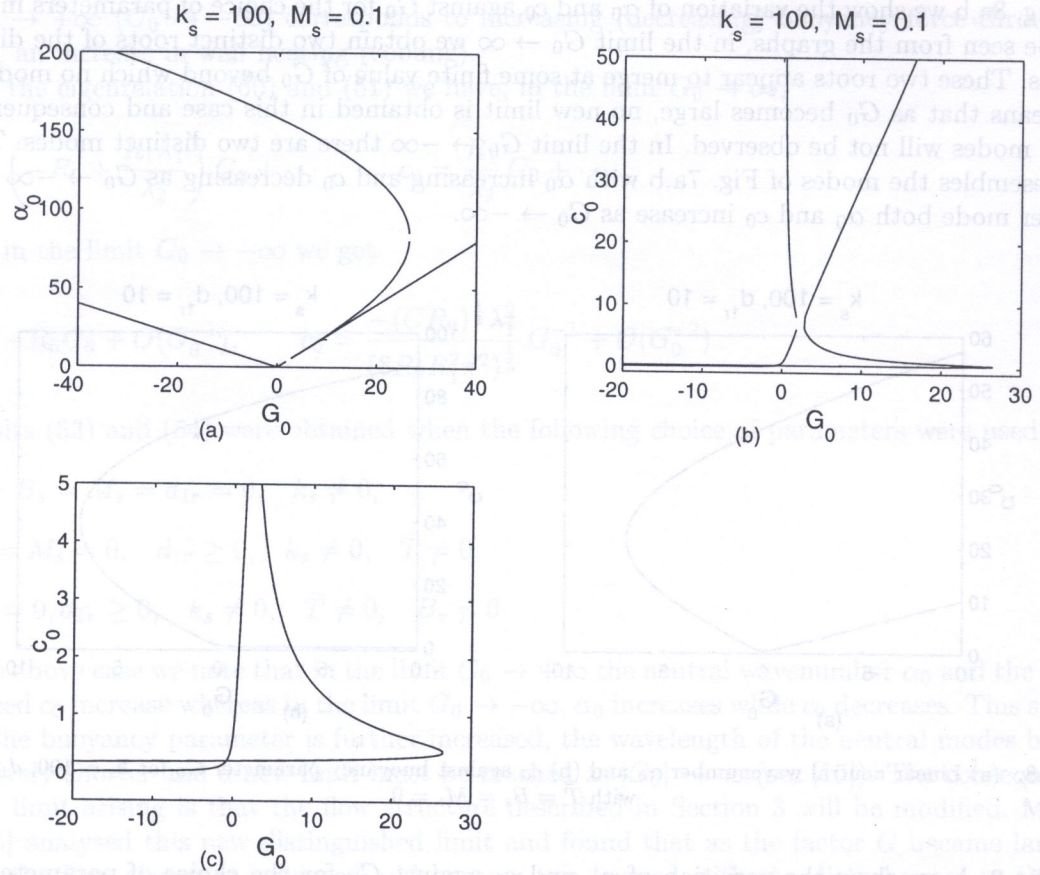

Fig. 9. (a) Linear neutral wavenumber α_0 and (b) c_0 against buoyancy parameter G_0 for $k_s = 100$, $M_s = 0.1$ with $d_{1r} = \bar{T} = B_s = 0$; (c) same as (b) but shown on a different scale

(iii) $\bar{T} = M_s = B_s = 0$, $d_{1r} \neq 0$, G_0 finite. In this case if $k_s \to \infty$, then $s_0 \to -\infty$ and one possibility is that α_0, c_0 remain $O(1)$ and approach their rigid wall values given by (55). Another possibility is that both α_0 and c_0 become large (see Fig. 2c,d), and are given by

$$\alpha_0 \sim \alpha_{01} k_s\,, \qquad c_0 \sim c_{01} k_s\,,$$

where

$$c_{01} = \frac{2\lambda_2 \pi}{-d_{1r}\lambda_1^3 \alpha_{01}}\,, \qquad \alpha_{01} = 2\left(1 + \sqrt{1 - \frac{2d_{1r}\lambda_1^2}{\lambda_2 \pi}}\right)^{-1}.$$

(iv) $d_{1r} \to \infty$. From the dispersion relations we find that both α_0, c_0 become large with

$$c_0 \sim \frac{\alpha_0}{\lambda_1}\,.$$

The precise limiting form depends on the value of $\bar{T}$, M_s, B_s, k_s, G_0. For instance, if $\bar{T} \neq 0$ and $M_s = B_s = 0$, $k_s \neq 0$, G_0 finite, then

$$\alpha_0 \sim \left(\frac{\lambda_1^2 d_{1r}}{-2\lambda_2 \pi \bar{T}^2}\right)^{\frac{1}{2}}.$$

If $\bar{T} \neq 0$, $B_s \neq 0$, $k_s \neq 0$ $M_s = 0$, G_0 finite, then we have

$$\alpha_0 \sim \left(\frac{\lambda_1^2 d_{1r}}{-2\lambda_2 \pi B_s^2}\right)^{\frac{1}{6}}.$$

If $\bar{T} \neq 0$, $B_s = 0$, $k_s \neq 0$ $M_s \neq 0$, G_0 finite, then

$$\alpha_0 \sim \left(\frac{\lambda_1^6}{-2\lambda_2 \pi M_s^2} \right)^{\frac{1}{3}} d_{1r}^{\frac{1}{6}}.$$

6. Summary

A systematic approach, based on a multi-deck disturbance structure of the flow, has been used to investigate the effects of heating and cooling on the stability of upper-branch Tollmien–Schlichting waves. We have extended the now well known theory of boundary layer flow over heated or cooled surfaces to include surface compliance.

By varying the buoyancy parameter G_0 in the range $-\infty < G_0 < \infty$ we were able to infer the effect of heating and cooling on the upper-branch Tollmien–Schlichting waves in boundary layer flow over a compliant surface. On the whole, buoyancy was found to be destabilizing to the boundary layer. Hall and Morris [10] and Mureithi et al. [15] arrived at the same conclusion in the rigid surface case.

When the linear neutral wavenumbers and wavespeeds were varied against the spring stiffness, k_s, tension, $\bar{T}$, and mass stiffness M_s parameters it was found noted that at least two modes exist. One of the modes is the rigid wall solution and the other modes arise because of the introduction of surface compliance. Among the compliant modes it was observed that the case $G_0 > 0$ led to wavenumbers and wavespeeds which are smaller than the wavenumbers and wavespeeds obtained when $G_0 = 0$. The case $G_0 = 0$ leads to wavenumbers and wavespeeds which are smaller than the modes obtained when $G_0 < 0$. This suggests that heating ($G_0 > 0$) leads to more stable compliant modes than the case where there is no heat transfer ($G_0 = 0$) which in turn leads to more stable compliant modes than the cooling case ($G_0 < 0$). In the case when α_0 and c_0 were varied against the damping parameter, d_{1r}, it was found that cooling leads to the most stable compliant mode followed by the $G_0 = 0$ case, with heating leading to the least stable compliant modes.

The analysis of the limiting cases where G_0 becomes large indicated that inviscid modes similar to the ones observed in the rigid surface case would be obtained. The analysis of this large G_0 limit was not done extensively in this work because it has been considered in detail in other previous studies (see for example [15]). The analysis of the limiting case where the damping, d_{1r} becomes large also pointed to the importance of a new Rayleigh structure for the flow with enhanced wavespeeds and shorter waves. Gajjar and Sibanda [9] arrived at the same conclusion in their study of the stability of channel flow over compliant surfaces. It is the intention of the authors to further investigate the new structures which are expected to arise when d_{1r} and some of the other parameters becomes large. Also the effects of heating and cooling on flow induced surface instabilities, and divergence are to be considered. It may also be interesting to move into the nonlinear regime and consider nonlinear effects.

Acknowledgements

Sandile Motsa gratefully acknowledges the financial support from the Norwegian Council of Universities, Committee for Cooperation Research and Development (NUFU).

Appendix

The integrals and constants appearing in the text are defined below. Here the ** in the integrals denotes that only the finite (Hadamard) part is taken.

$$I_0 = \int_0^{\infty **} U_B^2 \, dY, \qquad I_1 = \int_{Y_0}^{\infty **} \frac{1}{U_B^2} \, dY, \qquad I_2 = \int_{Y_0}^{0} \left(\frac{1}{U_B^2} - \frac{1}{\lambda_1^2 Y^2} + \frac{2\lambda_2}{\lambda_1^3 Y} \right) dY,$$

$$J_0 = \int_0^{\infty **} \theta_{By} \left(\int_{Y_0}^{Y_1} \frac{G_0 R_0 + \alpha_0 + G_0(\theta_B - R_0)}{U_B^2} \, \mathrm{d}Y_1 \right) \mathrm{d}Y,$$

$$J_1 = \int_{Y_0}^{\infty **} \frac{(\theta_B - R_0)}{U_B^2} \, \mathrm{d}Y,$$

$$J_2 = \int_{Y_0}^{0} \left[\frac{\theta_B}{U_B^2} - \frac{R_0}{\lambda_1^2 Y^2} + \left(\frac{2\lambda_2 R_0}{\lambda_1^3} - \frac{R_1}{\lambda_1^2} \right) \frac{1}{Y} \right] \mathrm{d}Y,$$

$$D_0 = \alpha_0^2 \lambda_1 \left[I_2 - \frac{1}{\lambda_1^2 Y_0} - \frac{\lambda_2}{\lambda_1^2} \right] - \frac{2\alpha_0 c_0 \lambda_2}{\lambda_1},$$

$$E_0 = \alpha_0^2 \lambda_1 \left(J_2 - \frac{R_0}{\lambda_1 Y_0} - \frac{\lambda_2 R_0}{\lambda_1} \right),$$

$$D_1 = \frac{2\alpha_0 c_0^2 \lambda_2}{\lambda_1^2} \left(\frac{c_0 \lambda_1}{s_0 - \lambda_1 c_0} \right) \left(\ln \left| \frac{c_0}{\lambda_1} \right| + 1 \right) + \frac{2\alpha_0 c_0^2 \lambda_2}{\lambda_1} \ln \left| \frac{c_0}{\lambda_1} \right|,$$

$$E_1 = \frac{-\alpha_0 R_1 c_0}{\lambda_1^2} \left[2 \ln \left| \frac{c_0}{\lambda_1} \right| + \frac{\lambda_1 c_0}{s_0 - c_0 \lambda_1} \ln \left| \frac{c_0}{\lambda_1} \right| + 2 + \frac{\lambda_1 c_0}{s_0 - c_0 \lambda_1} \right],$$

$$D_2 = \lambda_1 D_1 - c_0 D_0 + \alpha_0 c_1 \lambda_1 - \frac{\alpha_1 c_0 \lambda_1 s_0}{s_0 - c_0 \lambda_1} + \frac{(\alpha_1 c_0 + c_1 \alpha_0) \lambda_1^2}{s_0 - c_0 \lambda_1}$$
$$- \alpha_0 \left(1 - \frac{c_0 \lambda_1}{s_0} \right) \left[\alpha_0^2 I_0 - 2\alpha_0 c_0 - \alpha_0^2 I_1 \right],$$

$$E_2 = \lambda_1 E_1 - c_0 E_0 - \alpha_0 \left(1 - \frac{c_0 \lambda_1}{s_0} \right) \left[J_0 - \frac{\alpha_1}{\alpha_0} - \alpha_0 I_1 G_0 R_0 \right].$$

REFERENCES

[1] P.W. Carpenter, J.S.B. Gajjar. A general theory for two and three dimensional wall-mode instabilities in boundary layers over isotropic and anisotropic compliant walls. *Theoret. Comput. Fluid Dynamics*, **1**: 349–378, 1990.

[2] P.W. Carpenter, A.D. Garrad. The hydrodynamic stability of flow over Kramer type compliant surfaces. Part 1. Tollmien–Schlichting instabilities. *J. Fluid Mech.*, **155**: 465–510, 1985.

[3] P.W. Carpenter, A.D. Garrad. The hydrodynamic stability of flow over Kramer type compliant surfaces. Part 2. Flow-induced surface instabilities. *J. Fluid Mech.*, **170**: 199–232, 1986.

[4] P.W. Carpenter, P.J. Morris. Effect of anisotropic wall compliance on boundary layer stability and transition. *J. Fluid Mech.*, **218**: 171–223, 1990.

[5] C. Davies, P.W. Carpenter. Instabilities in plane channel flow between compliant walls. *J. Fluid Mech.*, **352**: 201–243, 1997.

[6] A.E Dixon, A.D. Lucey, P.W. Carpenter. Optimization of viscoelastic compliant walls for transition delay. *AIAA Journal*, **32**: 256–267, 1994.

[7] J.S.B. Gajjar. Nonlinear stability of nonstationery cross-flow vortices in compressible boundary layers. *Stud. Appl. Math*, **48**: 181–204, 1996.

[8] J.S.B. Gajjar, J.W. Cole. The upper-branch stability of compressible boundary layer flows. *Theoret. Comput. Fluid Dynamics*, **1**: 105–123, 1989.

[9] J.S.B. Gajjar, P. Sibanda. The hydrodynamic stability of channel flow compliant boundaries. *Theoret. Comput. Fluid Dynamics*, **8**: 105–129, 1996.

[10] P. Hall, H. Morris. On the instability of boundary layers on heated flat plates. *J. Fluid Mech.*, **245**: 367–400, 1992.

[11] L.M. Hocking. Non-linear instability of the asymptotic suction velocity profile. *Quart. J. Mech. Appl. Math*, **28**: 341–53, 1975.

[12] M.T. Landahl. On the stability of laminar incompressible boundary layer over a flexible surface. *J. Fluid Mech.*, **13**: 609–632, 1962.

[13] C.C. Lin. *The Theory of Hydrodynamic Stability.* Cambridge University Press, 1955.

[14] S.S. Motsa, J.S.B. Gajjar, P.S. Sibanda. On the upper-branch staybility of channel flows over compliant surfaces with heating/cooling. Submitted to *Eur. J. of Fluid Mech.*, 1999.

[15] E.W. Mureithi, J.P. Denier, A.K. Stott. The effect of buoyancy on upper-branch Tollmien–Schlichting waves. *IMA J. Appl. Maths.*, **58**: 19–50, 1997.

[16] F.T. Smith, R.J. Bodonyi. On the stability of the developing flow in a channel or circular pipe. *Q. J. Mech. Appl. Maths.*, **33**: 293–320, 1981.

[17] F.T. Smith, R.J. Bodonyi. Nonlinear critical layers and their development in streaming-flow stability. *J. Fluid. Mech.*, **118**: 165–185, 1982.

[18] F.T. Smith, K. Stewartson. On slot injection into a supersonic laminar boundary layer. *Proc. R. Soc. Lond.*, **A332**: 1–22, 1973.

[19] A.R. Wazzan, T. Okamura, A.M.O. Smith. The stability of water flow over heated and cooled flat plates. *J. Heat Transfer, Trans of the ASME*, 109–113, 1968.

[20] K.S. Yeo. The stability of boundary layer flow over single and multi-layer viscoelastic walls. *J. Fluid. Mech.*, **196**: 369–408, 1988.